行政院國家科學委員會專題研究計畫　成果報告

奈米材料的理論研究(2/2)

計畫類別：個別型計畫
計畫編號：NSC92-2113-M-032-010-
執行期間：92 年 08 月 01 日至 93 年 10 月 31 日
執行單位：淡江大學化學系

計畫主持人：王伯昌

計畫參與人員：王鴻偉、廖顯仁、林奕君、陳文豪、張詠昇

報告類型：完整報告

處理方式：本計畫可公開查詢

中　華　民　國 94 年 5 月 16 日

行政院國家科學委員會補助專題研究計畫 **■ 成 果 報 告**
□期中進度報告

奈米材料的理論研究(2/2)

計畫類別：■ 個別型計畫　　□ 整合型計畫
計畫編號：NSC 92-2113-M-032-010-
執行期間：　92　年 08 月 01 日 至　93　年　10 月　31 日

計畫主持人：王伯昌
共同主持人：
計畫參與人員： 王鴻偉、廖顯仁、林奕君、陳文豪、張詠昇

成果報告類型(依經費核定清單規定繳交)：□精簡報告　■完整報告

本成果報告包括以下應繳交之附件：
□赴國外出差或研習心得報告一份
□赴大陸地區出差或研習心得報告一份
□出席國際學術會議心得報告及發表之論文各一份
□國際合作研究計畫國外研究報告書一份

處理方式：除產學合作研究計畫、提升產業技術及人才培育研究計畫、列管計畫及下列情形者外，得立即公開查詢
□涉及專利或其他智慧財產權，□一年□二年後可公開查詢

執行單位：淡江大學化學系

中　華　民　國　94　年　1　月　31 日

Electronic Structure and Molecular Orbital Study of Hole Transport Material Triphenylamine Derivatives

Bo-Cheng Wang,
Department of Chemistry, Tamkang University, Tamsui, Taiwan 251,

Abstract

Recently, triphenylamine (TPA), 4,4'-bis(phenyl-*m*-tolylamino)biphenyl (TPD), 4,4'-bis(1-naphthylphenylamino)biphenyl (NPB) and their derivatives are widely used in the organic light emitting diode (OLED) devices as a hole transporting material (HTM) layer., We have optimized twenty different structures of HTM materials by using density functional theory (DFT), B3LYP/6-31G* method. All these different structures contain mono-amine and diamine TPA derivatives. The energies of HOMO and LUMO along with molecular orbitals for these HTMs were also determined. We have found that the central amine nitrogen atom and the phenyl ring, which is next to the central amine nitrogen atom, show significant contribution to the HOMO and LUMO, respectively. The sum of the calculated bond angles ($\alpha + \beta + \gamma$) of the central amine nitrogen atom, has been applied to describe the bonding and the energy difference for HOMO and LUMO in these TPA derivatives. Electronic structures calculations have been performed for these TPA derivatives. Again, the LCAO-MO patterns of HOMO and LUMO levels of these derivatives are used to investigate their electron density. The hole-transporting pathways are predicted for these compounds employing these calculated results.

Keywords: TPA, HTM, DFT and NPB.

* Corresponding author. E-mail address: bcw@mail.tku.edu.tw (B. C. Wang)

Introduction

During the past decade, the development of organic light emitting devices (OLED) has become one of the foremost topics in chemistry and applied physics.[1-7] Since a large number of organic materials exhibit high fluorescence quantum efficiencies in the visible region, the OLED should be used for the next generation of flat-panel display systems.[8-10] Unfortunately, these organic materials have low stability, insufficient luminescence efficiency and high driving voltage – the drawbacks that still remains to be overcome.

In order to improve the durability of the electro-luminescence (EL) devices, the multilayered EL devices have been proposed, which contain hole transporting materials (HTMs), electron transporting materials (ETMs) and the emitting layer.[1] Almost twenty years ago, Kodak group proposed HTM1 and HTM2 (Fig. 1) for the HTM materials and investigated the hole-transporting mechanism by means of the potential discharge techniques.[7] Then, chemist also developed a series of prototypical HTM materials, which include 4,4'-bis(phenyl-*m*-tolylamino)biphenyl (TPD) and 4,4'-bis(1-naphthylphenylamino)biphenyl (NPB) (Fig. 2).[8-14] All of these HTMs contain the triphenylamine (TPA) moiety, which has a central amine nitrogen atom connected to three phenyl rings (Fig. 3). Several studies have been carried out to investigate the TPA compound theoretically.[15-17] Pacansky *et al.* have used *ab initio* Hartree-Fock method with the 3-21G basis set to optimize geometric structures of TPA for both neutral and radical cation molecules, then, the hopping process between a neutral and an ionized TPA was predicted.[15] They have also concluded from an *ab initio* HF calculations that the unpaired electron is 59% localized on the central amine nitrogen atom of TPA.[15] The calculations showed that the central amine nitrogen atom significantly contributes to the highest occupied molecular orbital (HOMO). Then, Sakanoue *et al.* have reported a molecular orbital study of TPD, which is a

diamine compound.[18] They have made conclusion that the amine nitrogen atom and the phenyl ring of TPD are the main contributors to the HOMO and LUMO (the lowest unoccupied molecular orbital), respectively.[18] According to their theoretical calculation, the hopping process between a neutral and an ionized TPD has also been predicted.[18] NPB is another diamine HTM which has been applied in HTM widely; the electronic structure of NPB with various extra charges has been studied by means of the semiempirical PM3 and *ab initio* MO theories as well as by the DFT and TDOS methods by Zhang *et al.*[19] In particular, they have used the projection TDOS to investigate the electronic structures of individual atoms in NPB. The calculation results reveal that the central amine nitrogen atom in NPB has a significant contribution to HOMO. Such calculation is also found to be the same as that for the TPA compound.[19] Very recently, Lin *et al* generated the ionization potential, electron affinity and reorganization energies for TPA, NPB and TPD by using DFT B3LYP/6-31G* method.[16]

In general, most of HTM materials applied in electronic device contain the TPA moiety. In this study, we have considered twenty TPA derivatives of the TPA moiety, which are related to the HTM materials. First, we have generated the optimized geometric structure and the electronic structure of TPA by means of density functional theory (DFT). Then, the DFT method was applied to investigate the optimized structures and electronic structures for TPA derivatives (for mono-amine and diamine derivatives) systematically. The energies of molecular orbital levels for HOMO and LUMO are obtained by means of the DFT B3LYP/6-31G* calculation; these MOs are used to describe the electron density and to predict the possible hopping process (charge flowing mechanism) between the neutral and the radical cation of TPA compounds. Relations between the energy level of HOMO and LUMO and the optimized structures are also determined in these HTMs. In the hopping mechanism, it

has been observed that electron accepting molecules with strong affinity serve as the hopping sites in electron conductors, while the donor molecules with low ionization potential serve as the hopping sites in hole conductor. Thus, the molecular design for HTMs may consider the ionization potential, which is related to the energy levels of HOMO, and the optimized structure for this compound. In this study, we would like to provide more information concerning the energies and the optimized structures for TPA derivatives, which can be useful to improve and design new HTM materials.

Computations

The density functional theory (DFT) B3LYP method with the 6-31G* basis set has been used to generate the optimized structure for the ground state TPA and its derivatives. The calculated molecular orbitals, HOMO and LUMO were used to determine the electron density in these derivatives. The electron density was employed to investigate the charge flowing and hopping mechanism in these compounds. In the present study, twenty different compounds have been studied which contain mono-amine and diamine TPA derivatives. All the calculations have been performed using GAUSSIAN 03 program package.[20]

Results and discussion

Geometrical and electronic structures of TPA

The TPA molecule is composed of three phenyl rings with a central amine nitrogen atom; it could be visualized as a bladed propeller with C_3 symmetry. Fig. 3 shows the side and the top views of the optimized structure of TPA. The optimized geometric parameters of TPA are presented in Table 1. In particular, the central NC_3 fragment is an equivalent triangle and the C_3 axis goes through the central amine

nitrogen atom perpendicular to the NC_3 plane. The three dihedral angles between the NC_3 plane and the phenyl rings have the same value of 41.57° for the TPA compound.

To investigate the substitution effect in the central amine nitrogen atom of TPA, we used compounds I to VI (Fig. 4). We start with the NH_3 molecule, which is the amine group without any phenyl substitution. Then, the phenyl and methyl groups are added to these amine compounds. Compound II contains one amine nitrogen atom and three methyl substituents. Compounds III and IV both contain one phenyl ring and compound IV has two methyl substituents. For compounds V and VI, there are two and three phenyl substituents, respectively. All these compounds were optimized by the DFT B3LYP/6-31G* method. Table 2 shows the calculated three CNC bond angles (α, β and γ) and the sum of the calculated bond angles ($\alpha + \beta + \gamma$) of TPA derivatives based on the DFT optimized structures. For compounds I, II and III, the sum of the calculated bond angles ($\alpha + \beta + \gamma$) are about 317°, 334° and 340°, respectively. Thus, these three compounds have a pyramid structure, and the central amine nitrogen is an sp^3-hybridized atom. According to Table 2, the sum of the calculated bond angles ($\alpha + \beta + \gamma$) is closed to 360° for compounds IV, V and VI, since they have three phenyl substituents. This calculation showed that NC_3 is nearly planar and the central amine nitrogen is an sp^2-hybridized atom for these three compounds. The sum of the calculated bond angles ($\alpha + \beta + \gamma$) increases for these derivatives with the number of phenyl substituents in the central amine nitrogen atom. According to the molecular orbital analysis, compounds I, II and III have an sp^3 hybridization for the amine nitrogen atom and contain non-bonding electrons in the singlet ground state. For compounds IV, V and VI, the central amine nitrogen atom has an sp^2 hybridization and the non-bonding *2p* electrons; they have singlet ground state (Fig. 5). This calculation implies that these non-bonding electrons in the central amine nitrogen atom and the NC_3 planar structure of TPA derivatives may affect the

aggregation (intermolecular π-stacking) and the electron or hole hopping mechanism of the HTM materials.

The orbital energies of HOMO and LUMO are obtained by the B3LYP/6-31G* method for compounds I to VI (Table 3). The orbital energy of HOMO has been increased (from –6.78 eV to –5.00 eV) for compounds I to III with increasing the number of phenyl and methyl substituents in the central amine nitrogen atom of TPA derivatives, because the electron density in the central amine nitrogen atom may play an important role for HOMO. Compounds IV, V and VI have the planar NC_3; their orbital energies HOMO are around -5.00 eV. On the contrary, the orbital energy of LUMO has been decreased with increasing the number of phenyl substituent in these derivatives. Fig. 6 shows the MO diagram for the HOMO and LUMO of compounds I to VI. Comparing the MO diagrams of HOMO and LUMO, it can be seen that the electron cloud of the HOMO and the LUMO are concentrated on the central amine nitrogen atom and the phenyl substituents, respectively. Hence, it concludes that the most active site in this state is the central amine nitrogen atom and the phenyl ring for HOMO and LUMO. This result is also consistent with that of DOS calculations.[19]

According to the Mulliken population analysis (Table 4), 33% of electron density is distributed on the central amine nitrogen atom for the HOMO level of TPA and 22% electron density is distributed in the three-phenyl rings equally. Contrarily, more electrons are distributed on the three-phenyl rings (33% each) than on the central amine nitrogen atom (0.07%) for the LUMO level of TPA. This calculated results also indicated that the electrons in the HOMO level are more aggregated on the central amine nitrogen atom than on three phenyl rings whatever may be the substituents of TPA. Due to this electronic property, TPA has always been used as HTM materials.

In order to determine the hole-transporting mechanism in the TPA compound, the

MO diagram for HOMO and LUMO levels have been considered. The charge may flow from the central amine nitrogen (which contains more electron population) in neutral TPA via adjacent phenyl ring (which has less electron population) to the nitrogen in cation TPA. The B3LYP calculation was used to investigate the electronic and the geometrical structures for the neutral and the radical cation (hole) states of TPA. The calculation results reveal that the optimized structures changed slightly from the neutral to the hole state of TPA. The charge distribution for both the states is illustrated in Fig. 7. As seen in this figure, the charge of the nitrogen atom changes slightly (-0.651 to -0.561) for the two states as compared to the charge changed for the phenyl rings. This conclusion may support our proposed mechanism for the hole-transporting process in the TPA compound.

Geometrical and electronic structures of TPA derivatives

The alkyl group is added to the HTMs that could help to avoid an irreversible oxidation reaction and to increase the T_g (glass transition temperature) and the rigidity of the structure.[21,22] The experimental results also indicate that the alkyl substitution may affect the durability of HTM in the application of the EL devices.[21] Adachi et al. proposed that the dominant factor for obtaining high durability in organic EL devices is the ionization potential (I_p) of HTMs; it is related to the HOMO energy of the compound.[17] Thus, the alkyl group is substituted to the phenyl ring of TPA which may modify the HOMO energy. In the present work, the DFT method was used to investigate the effect of alkyl group substitution in the TPA derivatives with different substitution position and to study the relation between the optimized structure and the HOMO and LUMO energies in these derivatives.

According to our calculation, the sum of the calculated bond angles ($\alpha + \beta + \gamma$) and the phenyl substituent in TPA derivatives may affect the HOMO and LUMO

energies, respectively. In order to investigate the relation between the HOMO, LUMO energies and the optimized structure for these TPA derivatives, compounds VII – IX were proposed for the DFT calculation (Fig. 8). Compound VII has the bonding between two phenyl rings so that the connected phenyl rings are restricted to a more planar structure. Compound VIII has two phenyl rings connected by $–CH_2-$ from the TPA compound. For compound IX, two neighboring phenyl rings are connected by $–CH_2-$ group within C_2 symmetry. Tables 5 and 6 show the sum of the calculated bond angles ($\alpha + \beta + \gamma$), the dihedral angle ψ, ψ' and ψ'' (which are denoted in Fig. 8) and the orbital energy levels of HOMO and LUMO based on the structure optimized by DFT calculations. For these TPA derivatives, their sum of the calculated ($\alpha + \beta + \gamma$) bond angles are near 360°, thus, only the dihedral angle ψ, ψ' and ψ'' affect their HOMO and LUMO energies. According to the structure analysis, compounds VII, VIII and IX have two phenyl rings connected by a chemical bond or $–CH_2-$. We found that the dihedral angle between the phenyl ring and the NC_3 plane in the TPA derivatives may be the other major factor to affect the orbital energy of HOMO besides the sum of the calculated bond angles ($\alpha + \beta + \gamma$).

Furthermore, compounds X, XI and XII (Fig. 8) have the methyl group substituted in the *para*, *meta* and *ortho* position of each phenyl ring in TPA, respectively. These derivatives have been used to determine the substitution effect in the phenyl ring of TPA derivatives. Compounds X and XI represent the *para* and *meta* substitution in the phenyl ring of TPA; their methyl substituents affect slightly to the ψ. Thus, their HOMO energies change only 0.1 to 0.2 eV.

Compounds XIII, XIV, XV and XVI (Fig. 9) represent biphenyl substituted in one of the central amine nitrogen atom of TPA moiety; compounds XIV and XVI are the α- and β- substitution by the naphthalene in the amine nitrogen atom of compound XV. The calculated HOMO and LUMO energies for these compounds are

presented in Table 6. Thus, compounds XIII and XV are one phenyl group substitutions of compounds VII and VI, respectively. Comparing these two sets of compounds, we can see that the calculated HOMO and LUMO energies change slightly between compounds VI and XV, VII and XIII, respectively. Since the HOMO energy is related to the sum of the calculated ($\alpha + \beta + \gamma$) bond angles, these sums do not change between compounds VI (TPA) and XV. Thus, the HOMO energy in compound XV is close to that of TPA (-4.95 eV *vs.* -4.91 eV). A comparison of the HOMO and LUMO energies for compounds VI and XV shows 0.04 eV and 0.40 eV energy difference for the HOMO and LUMO levels, respectively. According to the above result, we suggest that the central amine nitrogen atom is the major contributor to the HOMO and the phenyl rings around the amine nitrogen atom are the major contributors for the LUMO. Compound XV has one more phenyl substituent than compound VI and its LUMO energy changes slightly as compared to that of compound VI. Similarly, compounds VII and XIII have the same HOMO and LUMO energy differences as those of compounds XV and VI. Compounds XIV and XVI are the α- and β- substitution by the naphthalene. Thus, the substitution position in naphthalene does not affect their HOMO and LUMO energies.

Diamine HTM materials and their electron structures

As far as we know, most of the HTMs in the OLED device contain the TPA moiety. For example, TPD and NPD are the diamine HTMs that contain two TPA moieties. In this study, the TPA moiety has been used and extended to TPD, NPD and other related diamine HTM materials investigating their relative physical properties.

According to the calculated results for TPA, the HOMO energy of TPA is related to the non-bonding electron of the central amine nitrogen atom for the TPA moiety and the LUMO energy for these compounds depends on the phenyl ring around the

central amine nitrogen atom.

In order to calculate HOMO and LUMO energies for these diamine HTMs, a series of diamine compounds were applied for this study. Compounds XIX, XVII and XX have one, two and three phenyl rings between two amine nitrogen atoms, respectively. Compound XVIII has the fluorene moiety between two amine atoms. In this study, the optimized structures and the orbital energies of HOMO and LUMO are obtained by the DFT method (Table 8). As seen in this table, the orbital energy of HOMO depends on the non-bonding electron of the amine nitrogen atom and π-electron conjugation between the two amine nitrogen atoms in these diamine derivatives. Since the phenyl ring affect the π-electron conjugation between two amine nitrogen atoms, compound XIX has one phenyl ring and it should increase the π-electron resonance and increase HOMO energy comparing to that of TPA (-4.65 eV *vs.* –4.95 eV). Compounds XVII and XX contain two and three phenyl rings between two amine nitrogen atoms but their phenyl rings are not located in the same plane; this may block the π-electron conjugation. Thus, the calculated HOMO energies decrease for these compounds (-4.73 eV and -5.30 eV). For compound XVIII, presence of the fluorine keeps the two phenyl ring in the same plane, so it enhances the π-electron conjugation and the HOMO energy is -4.63 eV, 0.32 eV higher than that of TPA. For the LUMO energy for these diamine derivatives, the DFT calculation show that the phenyl ring substituted in the central amine nitrogen plays a significant role in the LUMO orbital energy. The orbital energy of LUMO decreases with increasing the number of phenyl substituents between two amine nitrogen atoms. Thus, compound XX contain three phenyl rings between two amine nitrogen atoms and it has the lowest calculated LUMO energy (-0.98 eV) among these four derivatives. Compounds XVII and XVIV both have two phenyl rings and their LUMO energies have almost the same value (-0.86 eV and -0.81 eV).

Conclusion

According to the results described above, the central amine nitrogen atom and the phenyl ring in the TPA exhibit significant contributions to HOMO and LUMO respectively. Our calculated results also indicated that the HOMO energy for the TPA derivatives is related to the sum of the calculated bond angles ($\alpha + \beta + \gamma$) and the non-bonding electron of the central amine nitrogen. For the diamine HTMs, we conclude that the HOMO energy increase with increasing the number of phenyl rings between two amine nitrogen of diamine HTMs. On the contrary, the LUMO energy in these compounds increases with increasing the number of phenyl rings between two amine nitrogen of diamine HTMs. This relationship between the optimized structure and the HOMO and LUMO energies in these TPA related HTMs might provide more information to improve and to design new HTM materials.

Acknowledgment

We thank Prof. Alexander Mebel for reading the manuscript and the National Science Council of Taiwan, ROC for supporting this research.

References:

1. C. W. Tang, S. A. VanSlyke, Appl. Phys. Lett., 51 (1987), 913.
2. R. H. Young, C. W. Tang, A. P. Marchetti, Appl. Phys. Lett., 80 (2002), 874.
3. U. Talmach, H. Detert, H. Meier, V. Gebhardy, D. Haarer, A. Bacher, H. –W. Schmidt, Opt. Mater., 9 (1998), 77.
4. C. Adachi, T. Tsutsui, S. Tokito, Appl. Phys. Lett., 51 (1987), 913.
5. P. E. Burrows, S. R. Forrest, Appl. Phys. Lett., 64 (1994), 2285.
6. I. D. Parker, J. Appl. Phys., 75 (1994), 1656.
7. P. M. Borsenberger, W. Mey, A. Chowdrt, J. Appl. Phys., 49 (1978), 273.
8. B. Domercq, R. D. Hreha, Y. –D Zhang, N. Larribean, J. N. Haddock, C. Schultz, S. R. Marder, B. Kippelen, Chem. Mater., 15 (2003), 1491.
9. N. von Malm, R. Schmechel, H. von Seggern, Synth. Met. 126 (2002), 87.
10. Y. Shirota, Y. Kuwabara, H. Inada, T. Wakimoto, H. Nakada, Y. Yonemoto, S. Kawami, K. Imai, Appl. Phys. Lett., 67 (1994), 807.
11. I. G. Hill, A. Kahn, J. Cornil, D. A. dos Santos, J. L. Brédas, Chem. Phys. Lett., 317 (2000), 444.
12. R. Q. Zhang, C. S. Lee, S. T. Lee, Appl. Phy. Lett., 75 (1999), 2418.
13. Q. Haung, G. Evmenenko, P. Dutta, T. J. Marks, J. Am. Chem. Soc., 125 (2003), 14704.
14. G. Vamvounis, H. Aziz, N.-X. Hu, Z. D. Popovic, Synth. Met., 143(2004), 69.
15. J. Pacansky, R. J. Waltman, H. Seki, Bull. Chem. Soc. Jpn., 70 (1997), 55.
16. B. C. Lin, C. P. Cheng, Z. P. M. Lao, J. Phys. Chem. A, 107 (2003), 5241.
17. C. Adachi, K. Nagai, N. Tamoto, Appl. Phys. Lett., 66 (1995), 2679.
18. K. Sakanoue, M. Motoda, M. Sugimoto, S. Sakaki, J. Phys. Chem. A, 103 (1999), 5551.
19. R. Q. Zhang, C. S. Lee, S. T. Lee, J. Appl. Phys., 112 (2000), 8613.
20. M. J. Frisch, G. W. Trucks, H. B. Schlegel, G. E. Scuseria, M. A. Robb, J. R.

Cheeseman, V. G. Zakrzewski, J. A. Montgomery, R. E. Stratmann, J. C. Burant, S. Dapprich, J. M. Millam, A. D. Daniels, K. N. Kudin, M. C. Strain, O. Farkas, J. Tomasi, V. Barone, M. Cossi, R. Cammi, B. Mennucci, C. Pomelli, C. Adamo, S. Clifford, J. Ochterski, G. A. Petersson, P. Y. Ayala, Q. Cui, K. Morokuma, D. K. Malick, A. D. Rabuck, K. Raghavachari, J. B. Foresman, J. Cioslowski, J. V. Ortiz, B. B. Stefanov, G. Liu, A. Liashenko, P. Piskorz, I. Komaromi, R. Gomperts, R. L. Martin, D. J. Fox, T. Keith, M. A. Al-Laham, C. Y. Peng, A. Nanayakkara, C. Gonzalez, M. Challacombe, P. M. W. Gill, B. G. Johnson, W. Chen, M. W. Wong, J. L. Andres, M. Head-Gordon, E. S. Replogle, J. A. Pople, Gaussian 03, Gaussian, Inc., Pittsburgh, 2003.

21. H. Inada, Y. Shirota, J. Mater. Chem. 3 (1993), 319.
22. Y. Kuwabara, H. Ogawa, H. Inada, N. Namo, Y. Shirota, Adv. Mater., 6 (1994), 667.

Figure Caption:

Fig. 1 Chemical structures of HTM1 and HTM2

Fig. 2 Chemical structures of TPD, TTB and NPB

Fig. 3 Top and side views of optimized TPA

Fig. 4 Molecular structures of compounds I – VI

Fig. 5 sp^2 and sp^3 bonding orbitals for the central amine nitrogen of TPA

Fig. 6 Molecular orbitals HOMO and LUMO for compounds I - VI

Fig. 7 Charge distribution for the neutral and cation states of TPA

Fig. 8a Optimized geometrical structures of compounds VII – XII

Fig. 8b Molecular structures of compounds VII – XII

Fig. 9a Optimized geometrical structures of compounds XIII – XX

Fig. 9b Molecular structures of compounds XIII – XX

Fig. 10 Molecular orbitals HOMO and LUMO for compounds XIII – XX

Table 1 Calculated geometrical parameters of TPA*

	Atomic label	DFT B3LYP/6-31G*
Bond Length (Å)	N1-C2	1.420
	C2-C3	1.400
	C3-C5	1.390
	C5-C7	1.390
Bond Angle (deg)	C2-N1-C8	119.99
	N1-C2-C3	120.56
	C2-C3-C5	120.46
	C3-C5-C7	120.62
	C5-C6-C7	119.15
Dihedral Angle (deg)	C8-N1-C2-C3	41.57
	N1-C3-C3-C5	179.57
	C2-C3-C5-C7	0.84

*The notation (numbering) of atoms is shown in Fig. 3.

Table 2 Calculated bond angle (α , β and γ) (degree) and sum of the calculated bond angles (α + β + γ) (degree) for compounds I to VI

	DFT B3LYP/6-31G*			
	α	β	γ	(α + β + γ)
I	105.75	105.75	105.75	317.25
II	111.55	111.55	111.55	334.65
III	111.02	114.59	114.59	340.20
IV	117.76	121.31	121.30	360.37
V	121.01	117.04	118.79	356.84
VI	120.08	119.99	119.91	359.98

Table 3 Calculated HOMO (eV) and LUMO (eV) energies for compounds I to VI

	DFT B3LYP/6-31G*	
	HOMO	LUMO
I	-6.87	2.14
II	-5.64	2.29
III	-5.39	0.25
IV	-5.02	0.37
V	-5.04	-0.16
VI	-4.95	-0.30

Table 4 DFT calculated molecular orbital coefficients of HOMO and LUMO for TPA compound.*

Atom	HOMO			LUMO		
	$\sum C_i^2$	MO proportion (%)		$\sum C_i^2$	MO proportion (%)	
N1	0.247	32.93	32.93	0.009	0.78	0.78
C2	0.02	2.66	22.38	0.01	0.87	32.93
C3	0.045	6		0.089	7.74	
C4	0.004	0.53		0.095	8.25	
C5	0.05	6.66		0.002	0.17	
C6	0.004	0.53		0.1	8.69	
C7	0.045	6		0.083	7.21	
C8	0.02	2.66	22.38	0.01	0.87	33.36
C9	0.004	0.53		0.1	8.69	
C10	0.05	6.66		0.002	0.17	
C11	0.004	0.53		0.1	8.69	
C12	0.045	6		0.086	7.47	
C13	0.045	6		0.086	7.47	
C14	0.02	2.66	22.38	0.01	0.87	32.93
C15	0.045	6		0.089	7.74	
C16	0.004	0.53		0.095	8.25	
C17	0.05	6.66		0.002	0.17	
C18	0.004	0.53		0.1	8.69	
C19	0.045	6		0.083	7.21	

*The notation (numbering) of atoms is shown in Fig. 3.

Table 5 Calculated bond angle (degree) and sum of the calculated bond angles (degree) for compounds VI to XII

DFT B3LYP /6-31G*	Bond Angle				Dihedral Angle		
	α	β	γ	(α + β + γ)	ψ	ψ’	ψ’’
VI	120.08	119.99	119.99	359.98	41.06	41.61	42.02
VII	125.82	125.81	108.36	359.99	56.08	1.68	1.67
VIII	120.29	119.08	119.08	358.45	82.93	5.55	5.55
IX	121.52	120.37	116.74	358.63	87.33	69.73	16.35
X	120.05	119.99	119.94	359.98	41.66	41.52	41.01
XI	120.03	120.02	119.93	359.98	42.31	42.51	41.89
XII	117.77	117.67	117.66	353.10	44.19	44.10	44.47

Table 6 Calculated HOMO (eV) and LUMO (eV) of compounds VI to XVI

	B3LYP/6-31G*	
	HOMO	LUMO
VI	-4.95	-0.30
VII	-5.33	-0.65
VIII	-4.93	-0.39
IX	-5.07	-0.32
X	-4.72	-0.23
XI	-4.84	-0.23
XII	-5.14	-0.20
XIII	-5.30	-0.98
XIV	-4.89	-1.03
XV	-4.91	-0.75
XVI	-4.94	-1.14

Table 7 Calculated HOMO (eV) and LUMO (eV) of compounds XVII to XX

	B3LYP/6-31G*	
	HOMO	LUMO
XVII	-4.73	-0.81
XVIII	-4.63	-0.86
XIX	-4.65	-0.44
XX	-5.30	-0.98

Fig. 1

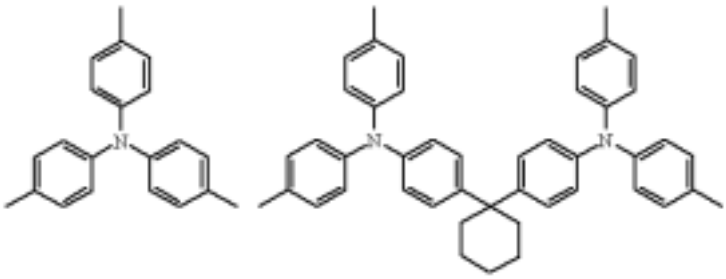

HTM 1 HTM 2

Fig. 2

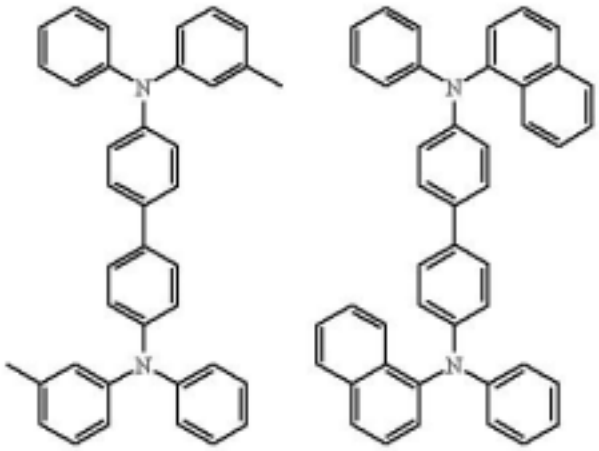

Fig. 3

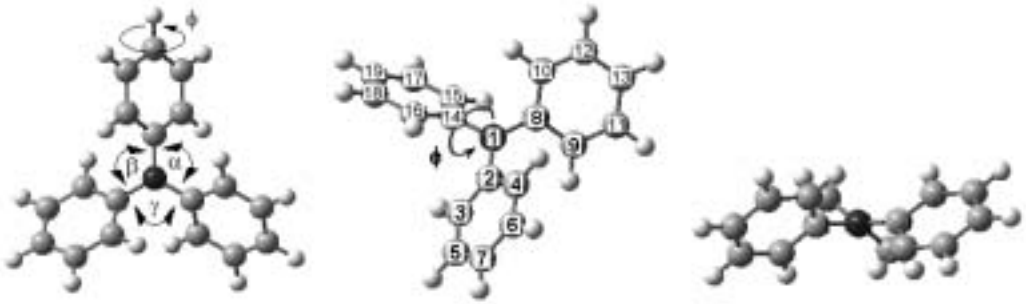

Molecular structure of TPA Top view of TPA Side view of TPA

]

Fig. 4

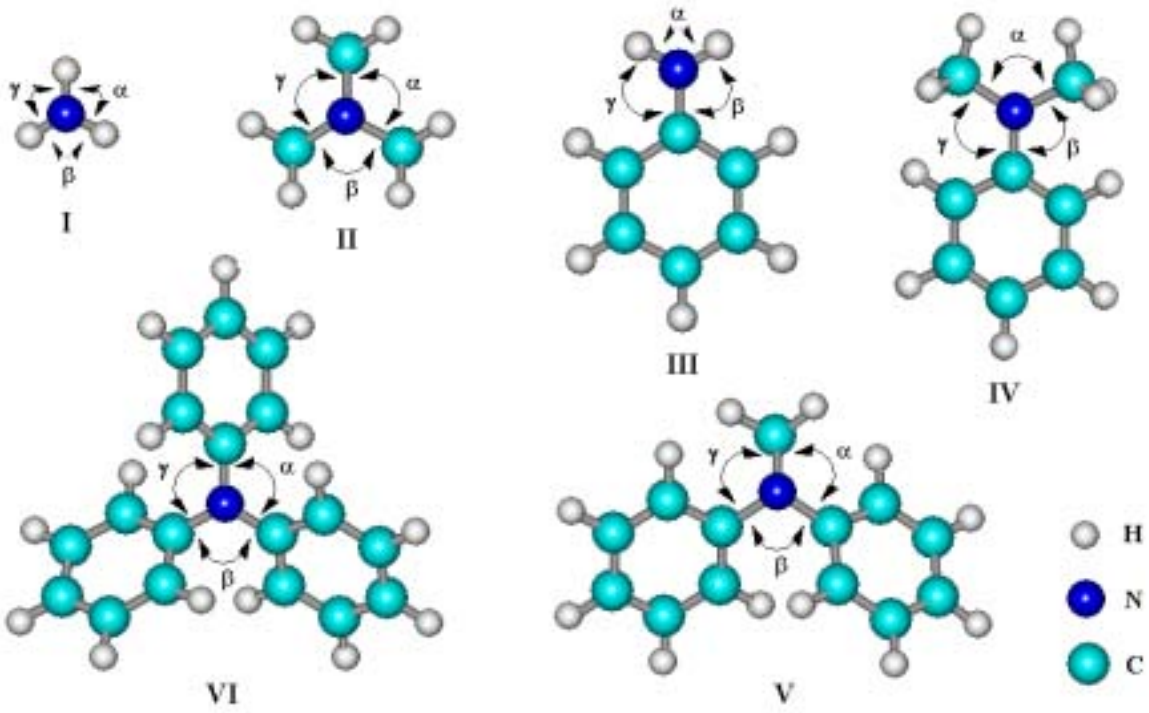

Fig. 5

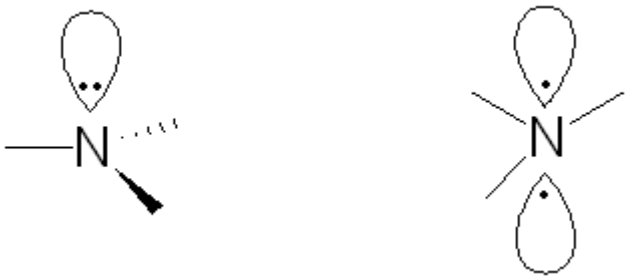

Fig. 6

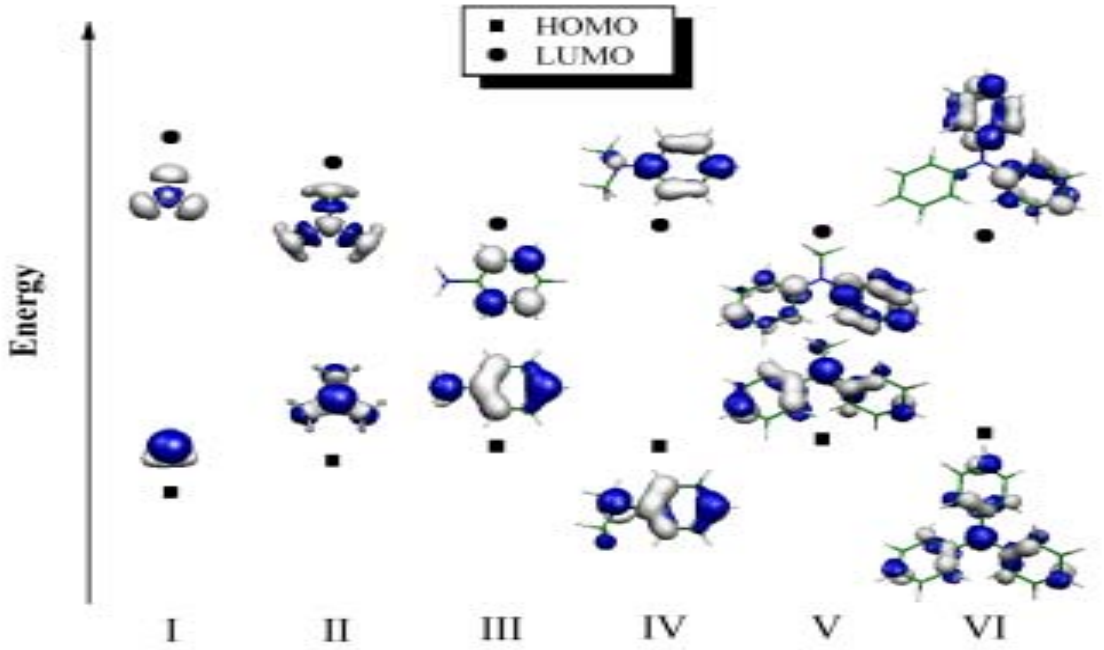

Fig. 7

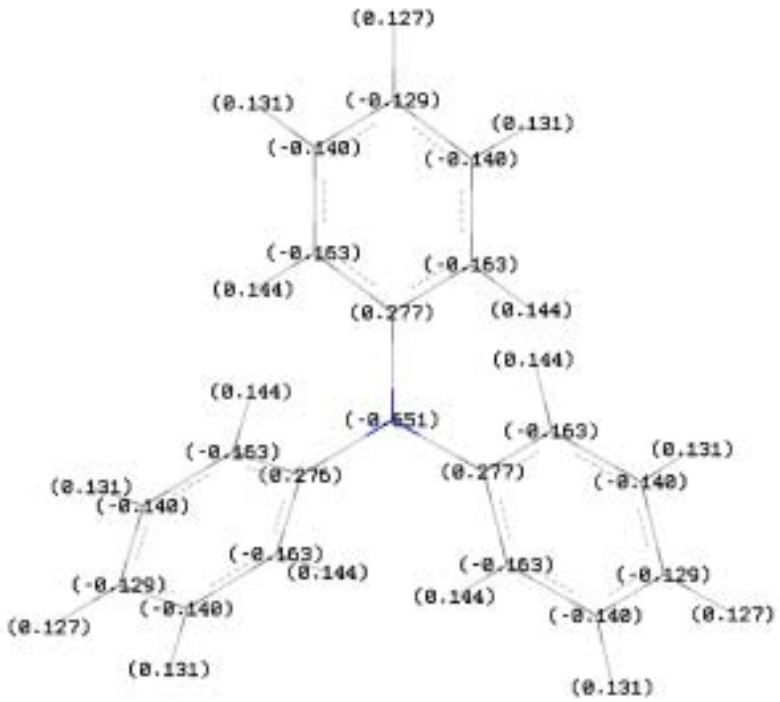

Neutral

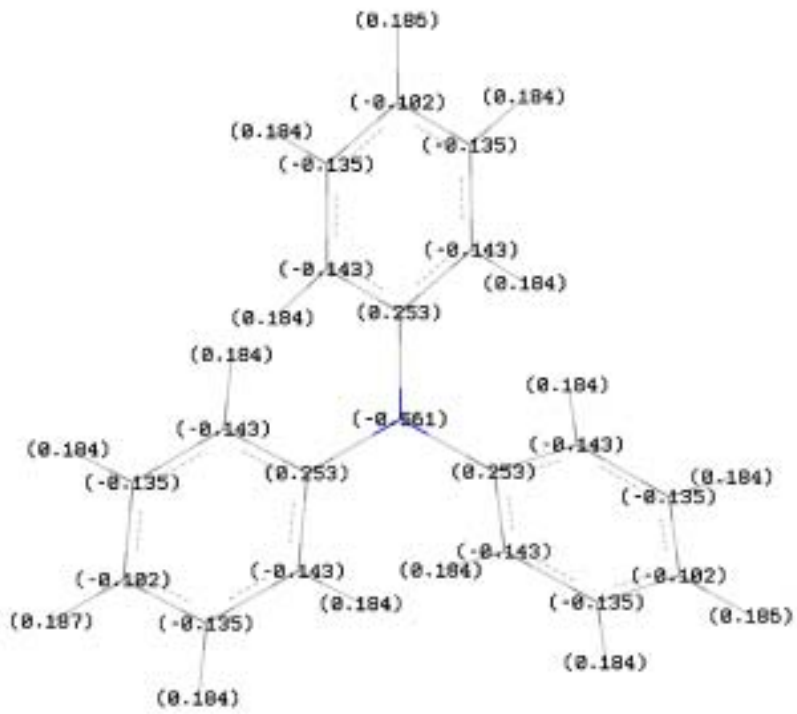

Cation

Fig. 8a

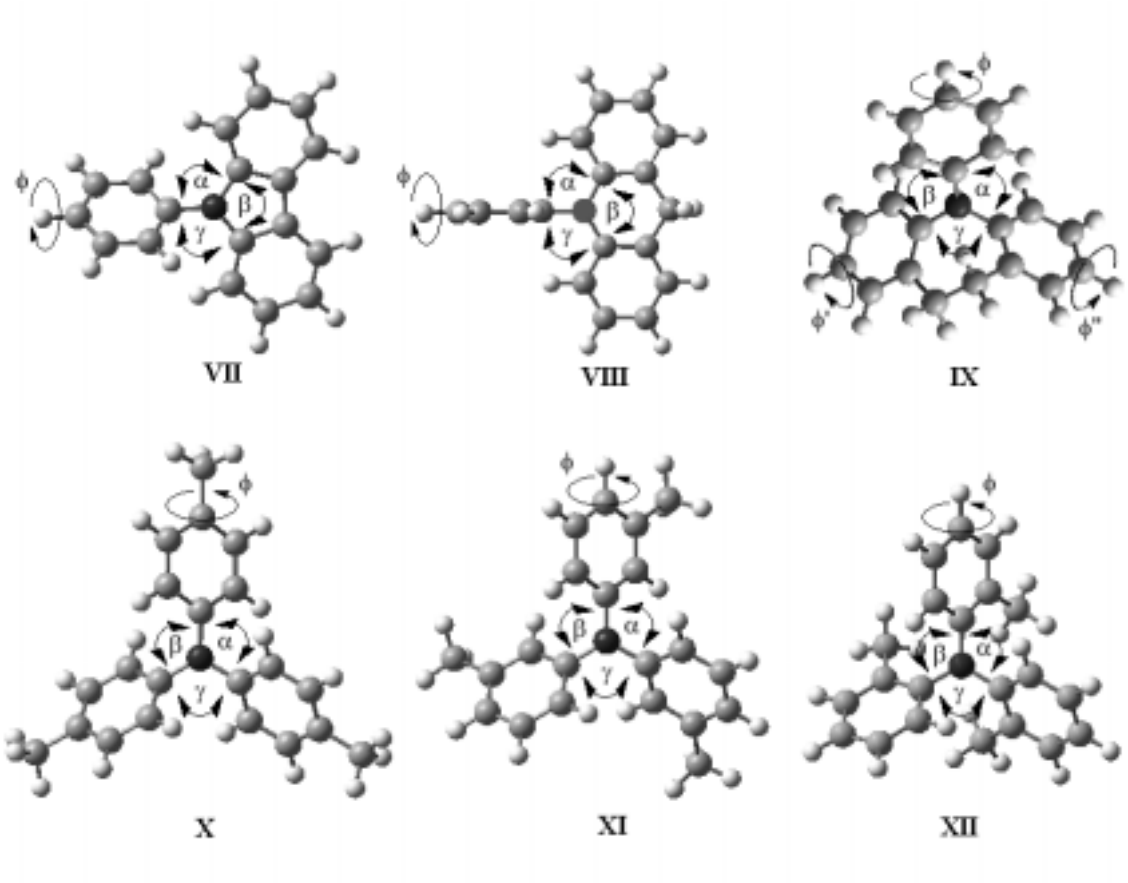

Fig. 8b

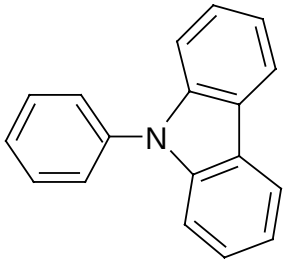

VII

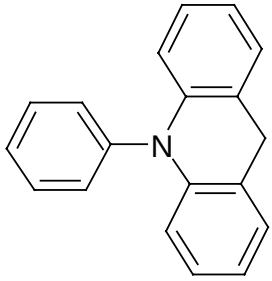

VIII

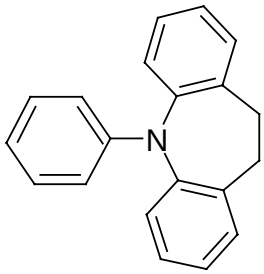

IX

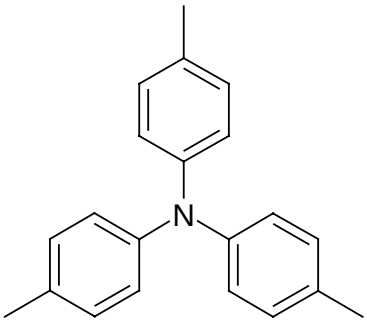

X

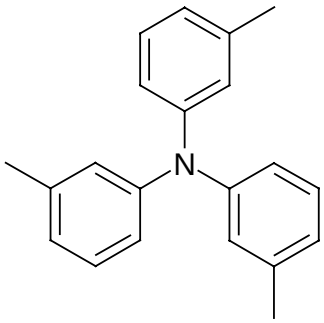

XI

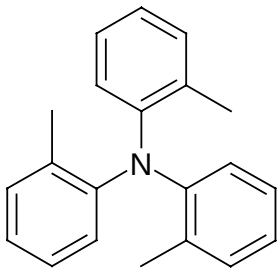

XII

Fig. 9a

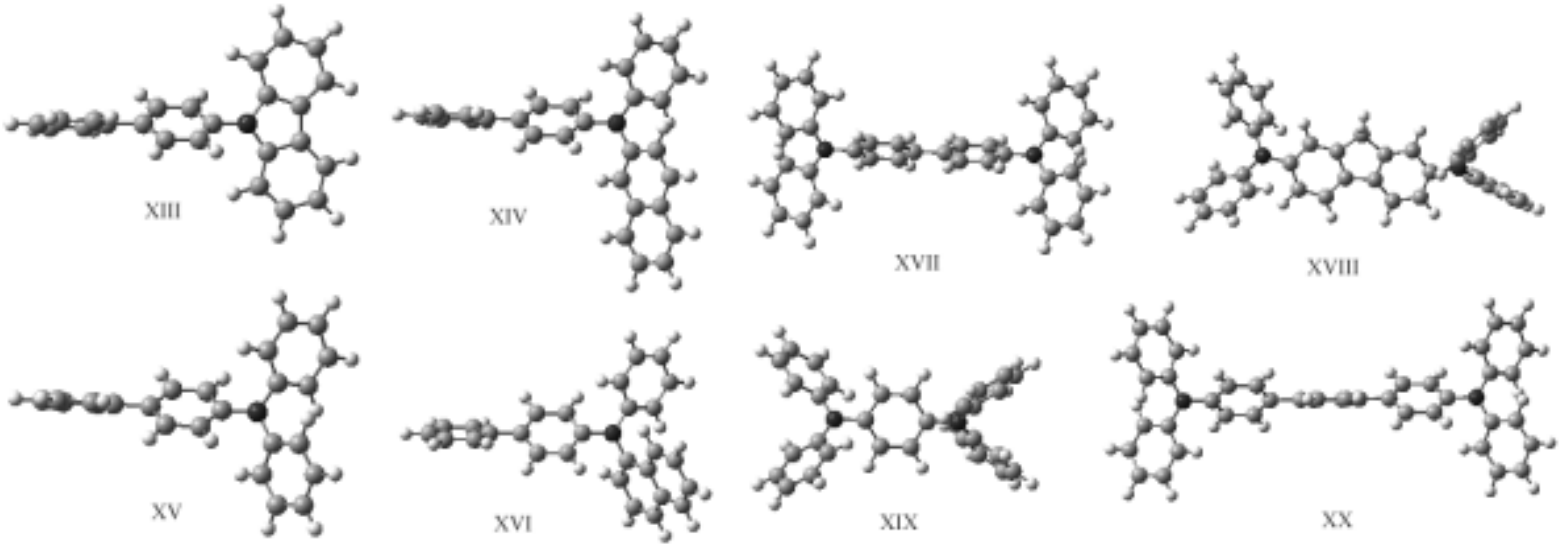

Fig.9b

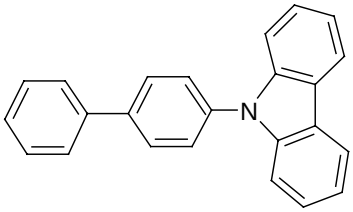

XIII

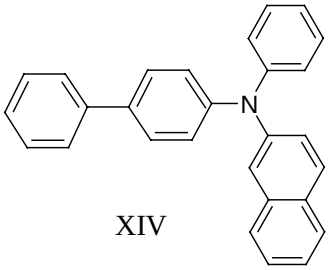

XIV

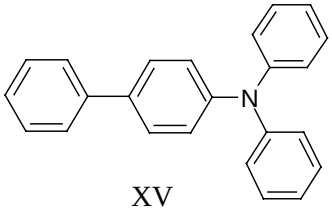

XV

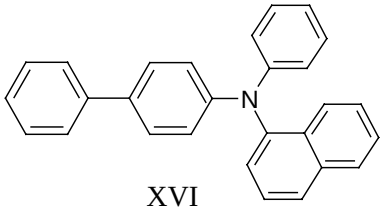

XVI

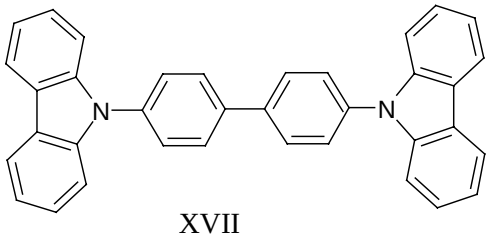

XVII

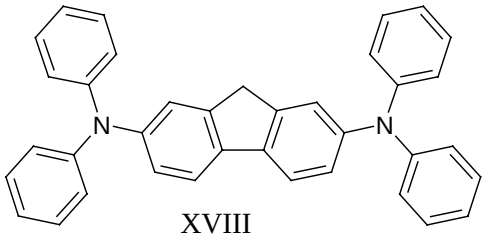

XVIII

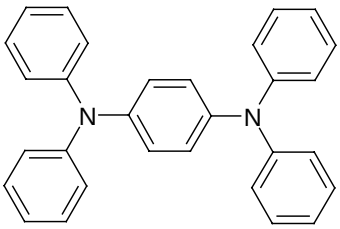

XIX

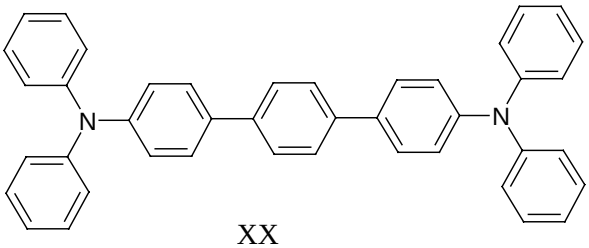

XX

Fig. 10

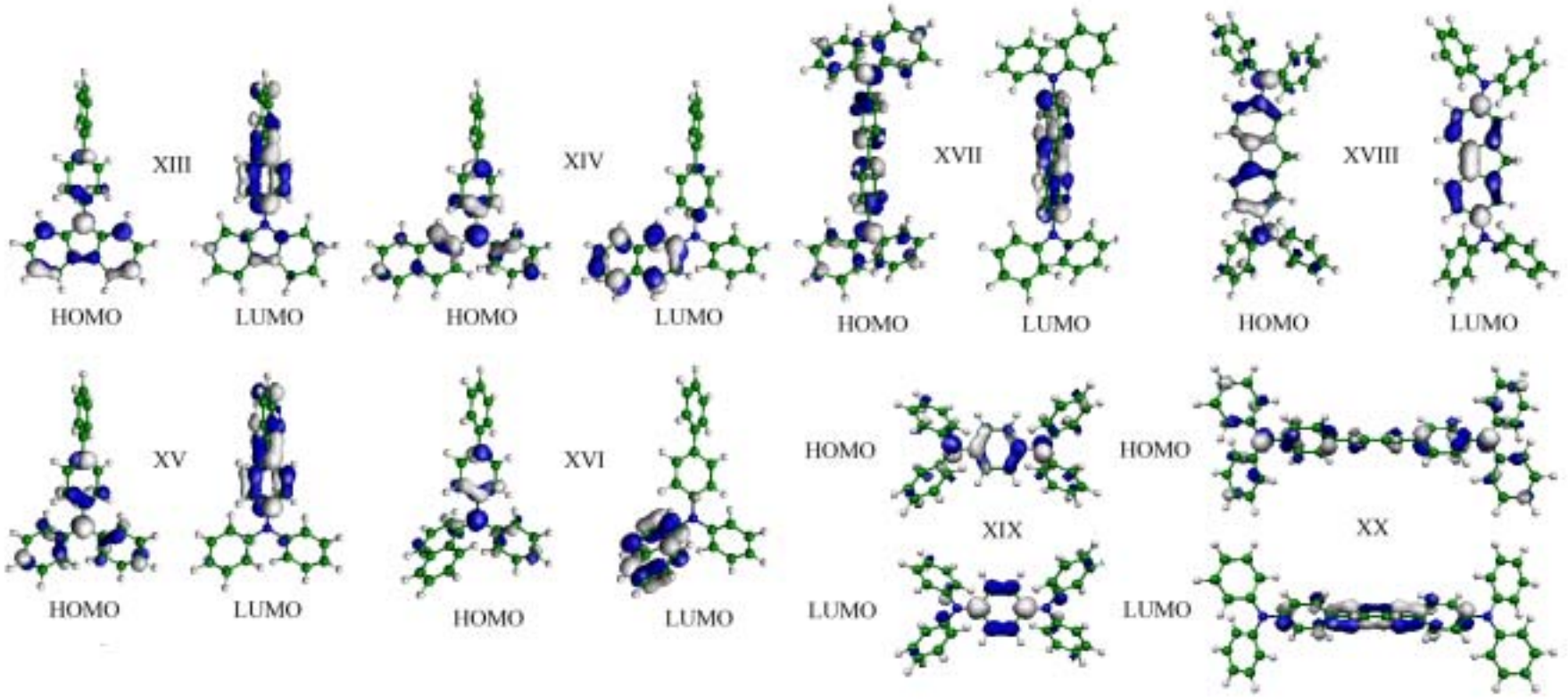
XIII
HOMO
LUMO
XIV
HOMO
LUMO
XVII
HOMO
LUMO
XVIII
HOMO
LUMO
XV
HOMO
LUMO
XVI
HOMO
LUMO
HOMO
XIX
LUMO
HOMO
XX
LUMO